Transcritical high-temperature heat pump with hydrocarbon mixtures – experimental setup and model predictions

T. Pfeiffer[a,b,*], C. Arpagaus[a], S. Bertsch[a], L. Brendel[a], M. Wördemann[b], C. Thomas[b]

[a]*OST – Eastern Switzerland University of Applied Sciences, Institute for Energy Systems, Buchs SG, Switzerland*
[b]*Dresden University of Technology, Schaufler Chair of Refrigeration, Cryogenics and Compressor Technology, Dresden, Germany*

Abstract

Industrial heat pumps must often overcome large temperature changes in the heat sink and heat source. Transcritical heat pump cycles with pure refrigerants can adapt to the temperature change in the heat sink but always have a constant temperature during evaporation. Transcritical refrigerant mixtures give an additional degree of freedom: The saturation temperature changes during evaporation and can match the heat source temperature change in counterflow configuration. This allows for independent temperature glide matching between the heat source and the heat sink. To verify this additional degree of freedom experimentally, a customized transcritical high-temperature heat pump prototype with 20 kW heating capacity was built and is introduced in this paper. A thermodynamic model of the heat pump is described and applied to an example application with source inlet and outlet temperatures of 90 °C and 60 °C and sink inlet and outlet temperatures of 100 °C and 150 °C, respectively. The model predicts a coefficient of performance (COP) improvement of over 10% and a volumetric heating capacity (VHC) improvement of over 50% for the best-performing R-290/R-601a refrigerant mixture compared to pure R-600a. The results encourage experimental verification as a basis for a pilot plant installation in an industrial environment.

Keywords: High-temperature heat pump; transcritical cycle; hydrocarbon mixtures; glide matching

1. Introduction

High-temperature heat pumps (HTHPs) can supply renewable heat, thereby supporting the decarbonization of industrial processes [1]. For applications with large temperature changes on the heat sink side like drying or heating in food preparation or paper production, heat pumps operating with isothermal condensation generally achieve lower efficiencies than transcritical cycles, which provide a better temperature match. By absorbing heat through evaporation in the subcritical two-phase region and rejecting heat in the supercritical region, transcritical cycles can deliver temperature changes of 100 K or more in the heat sink while maintaining high efficiencies [2].

When the heat source has a low mass flow rate or must be cooled significantly, the resulting large temperature change of the heat source medium reduces the performance of transcritical heat pumps using pure refrigerants, because the source outlet temperature pushes the evaporation temperature lower. Refrigerant mixtures can mitigate this mismatch by adapting their temperature glide during evaporation to the source temperature change. Therefore, transcritical cycles with refrigerant mixtures provide an additional degree of freedom, as the temperature glides of the evaporator and gas cooler can be adjusted independently.

While several theoretical studies on transcritical HTHPs exist, only three published experimental transcritical HTHP setups use refrigerants (R-32, R-1234ze(E), R-600) other than R-744 (CO_2) [2] (see Table 1). The references [3], [4], and [5] are theoretical studies, while [6], [7], [8], [9] and [10] are experimental studies. Notably, [6] and [7] are from the same experimental transcritical HTHP setup using synthetic refrigerants. The coefficient of performance (COP) is greater than 3 for all experimental studies, even for the one with a heat sink temperature change of 100 K [9]. The largest experimentally investigated source temperature change was 21 K. Higher values are needed to represent a broader range of industrial applications. Moreover, no experimental study has yet investigated the use of refrigerant mixtures.

Table 1. Results from simulations (theoretical) and experiments on transcritical high-temperature heat pumps (-: not available).

	Reference	Refrigerant	$T_{so,in}$	$T_{so,out}$	ΔT_{so}	$T_{si,in}$	$T_{si,out}$	ΔT_{si}	COP	VHC
		[-]	[°C]	[°C]	[K]	[°C]	[°C]	[K]	[-]	[kJ/m^3]
Simulations (theoretical)	Arpagaus et al. (2020) [2]	R-600	80	75	5	100	200	100	3	6’451
			30	25	5	30	200	170	2.9	2’678
		R-601	80	75	5	100	200	100	3.3	2’922
			30	25	5	30	200	170	2.9	916
	Udroiu et al. (2024) [3]*	R-1336mm(Z)	100	-	-	100	180	80	7	-
			100	-	-	100	250	150	3.3	-
	Vieren et al. (2023) [4]**	R-601	100	-	-	140	210	70	3.28	3’371
			115	-	-	116	202	86	4.2	4’746
			100	-	-	95	205	110	4.03	4’009
		R-601a	100	-	-	140	208	68	3.26	3’878
			115	-	-	116	202	86	4.26	5’456
			100	-	-	95	205	110	4.14	4’727
	Zhao et al. (2024) [5]	R-600	88	-	-	80	200	120	3.25	-
		R-1233ze(E)	88	-	-	80	200	120	3.57	-
		R-1336mzz(Z)	88	-	-	80	200	120	3.44	-
Experiments	Besbes et al. (2015) [6]	R-32	60	50	10	60	120	60	3.7 to 4.1	-
	Abi Chahla et al. (2019) [7]	R-1234ze(E)	82	61 to 69	13 to 21	100	150	50	3.3 to 3.7	-
	Kimura et al. (2018) [8], Saito (2017) [9]	R-600	80	-	-	80	180	100	>3.5	-
	Verdnik et al. (2019) [10]**	R-600	80	75	5	100	170	70	3.42	-

*with $T_{evap} = T_{so,in}$ and $T_{gc,out} = T_{si,in}$; **with internal heat exchanger

To address these research gaps, this study presents a transcritical HTHP prototype designed to test both pure refrigerants and refrigerant mixtures with adjustable compositions. Its performance is simulated for an industrial application featuring a 50 K temperature change on the heat sink and a 30 K temperature change on the heat source to prepare an experimental campaign.

2. Methodology

2.1. Experimental setup

To investigate refrigerant mixtures in a transcritical cycle, a customized HTHP prototype was developed. Fig. 1 shows the Piping and Instrumentation Diagram (P&ID) alongside a photograph of the final prototype (before insulation was applied). The components are listed in Table 2. As off-the-shelf components for hydrocarbons are usually not rated for pressures above the critical point, CO_2-compatible components were used to withstand supercritical pressures. For components such as the oil separator, expansion valves, heat exchangers, receiver, and suction accumulator, this poses no limitation. However, using a CO_2-rated compressor with hydrocarbons is expected to have an impact on the compressor efficiencies, since fluid properties strongly influence compressor efficiencies [11], [12].

Temperatures are measured by thermocouples at all locations except at gas cooler inlets and outlets, where Resistance Temperature Detectors (RTDs) are used for higher accuracy (marked in orange in Fig. 1). Both these RTDs and the thermocouples measuring suction, discharge, receiver inlet, low-pressure expansion valve inlet and outlet, and evaporator outlet were calibrated over the range of -23 °C to +110 °C using four high-accuracy RTDs (±0.05 K) immersed in a glycol bath. For temperatures exceeding the maximum allowable temperature of the calibration device (110 °C), the temperature sensors were not calibrated. The resulting accuracies of the temperature sensors are shown in Table 2. The pressure sensors are thermally decoupled from the pipes via flexible capillary hoses.

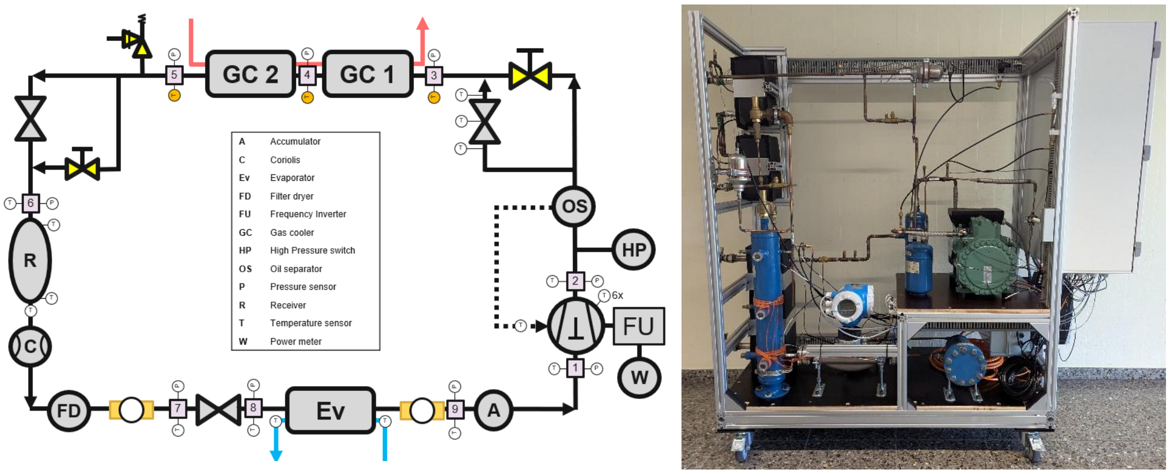

Figure 1. P&ID and photograph of the transcritical high-temperature heat pump prototype (without isolation).

On the heat sink side, two gas coolers were installed in series to enable the insertion of temperature and pressure sensors between the gas coolers in order to get more information on the non-isothermal gas cooling process.

The HTHP prototype uses two expansion valves: one positioned upstream of the evaporator to control the superheat, and a second downstream of the gas coolers to control the gas cooler outlet pressure, since an optimal supercritical pressure exists to maximize the COP [2, 13].

Table 2. Components used in the transcritical high-temperature heat pump prototype.

Component	**Model type**	**Manufacturer**	**Description (max. allowed temperature, pressure), measuring range and accuracy**
Compressor	2DME-7K	Bitzer	9.2 m^3/h at 50 Hz (max. 100 °C suction, 160 °C discharge, 10’000 kPa suction and discharge), PAG oil: Reniso LPG 150
Frequency inverter	FNY +30-4	Bitzer	-
Gas cooler	B4THx20/1P-NC-U	SWEP	Plate heat exchanger (max. 200 °C, 11’500 kPa)
Evaporator	B80ASHx24/1P-SC-M	SWEP	Plate heat exchanger (max. 200 °C, 3’700 kPa)
Oil separator	OS-16-CD	ESK Schultze	Oil volume: 0.6 L (max. 140 °C, 5’300 kPa)
Filter dryer	FT1-DN25-CDH	ESK Schultze	Replaceable solid core (max. 70 °C, 13’000 kPa)
Sight glass	3940/5	Castel	With dry/moisture indicator (max. 120 °C, 5’000 kPa)
Liquid receiver	OSA-5-CDH	ESK Schultze	Volume 5 L (max. 100 °C, 13’000 kPa)
Suction line accumulator	FA-22U-CDH	ESK Schultze	Volume 2.5 L (max. 100 °C, 10’000 kPa)
Expansion valve	MVL702.16-16-0.4	Siemens	K_{VS} = 0.4 m^3/h, magnetic actuator (max. 130 °C, 5’000 kPa)
Safety pressure switch	MBC 5100	Danfoss	Set to trip at 8’000 kPa discharge pressure
Pressure sensors	PAA-21Y (piezoelectric)	Keller	0 to 4’000 kPa and 10’000 kPa (max. 120 °C), max. ±1.5% of full scale
Thermocouples	Type K (class 2)	Alphasol Tec	-200 to +1250 °C, ±2.2 K, most were calibrated up to 110 °C with high-accuracy RTDs (±0.05 K), according to Section 2.1
RTDs	P-M-A-3-50-0-T-2	OMEGA	Class A, ±0.37 to ±0.55 K (depending on reading), calibrated up to 110 °C with high-accuracy RTDs (±0.05 K)
Power transmitter	ITL-101	Infratek	Expanded by the current sensor module to 0 to 75 kW range, 0.2% of the measuring range + 0.1% of the reading
Mass flow meter	Promass F 300	Endress+Hauser	Mass flow: ±0.10%, density: ±0.5 kg/m^3 (max. 150 °C)

2.2. Simulation model

The simulation model aims to simulate both a subcritical and a transcritical cycle for the same input parameters and select the one with the higher COP. A generic compressor correlation from Brendel et al. [14] was used to estimate the overall isentropic efficiency (η_{ois}) and volumetric efficiency (η_{vol}) based on suction and discharge pressures. The pressure losses (ΔP_{ij}) were assumed to be constant and set to values based on the pressure loss measurements from the commissioning of the prototype. This is a simplified assumption and can be improved by an empirical correlation after the collection of experimental data with the HTHP prototype.

Using the variable input parameters listed in Table 3, the model can be solved. The simulation model is programmed and executed in Python and all solvers in this model utilize the least squares method from the SciPy optimization library [15]. Property data are retrieved from REFPROP [16].

Table 3. Input parameters of the simulation model with the application example used in this study.

Input parameters	**Refrigerant**	$T_{\mathrm{so,in}}$	$T_{\mathrm{so,out}}$	ΔT_{so}	$T_{\mathrm{si,in}}$	ΔT_{sh}	ΔT_{sc}	$\Delta T_{\mathrm{pp,gc}}$	$\Delta T_{\mathrm{pp,e}}$	f_{comp}	V_{swept}
Example	Various	90 °C	60 °C	100 °C	150 °C	10 K	5 K	5 K	5 K	50 Hz	51 cm^3

The only two unknowns required to calculate both subcritical and transcritical cycles are the suction and discharge pressures, P_{suc} and P_{dis}. In subcritical mode, a solver iterates these pressures until the specified pinch point temperature differences are met in both evaporator and condensers. In transcritical mode, a first solver determines the suction pressure by satisfying the evaporator pinch point temperature difference, while a second solver iterates the discharge pressure until the maximum COP is achieved, ensuring the gas cooler pinch point temperature difference is also maintained. With the pressures set, all state points in both subcritical mode and transcritical mode can be computed.

In subcritical mode, the model calculations are straightforward. The condenser outlet is calculated from the specified subcooling value, the upper expansion valve is bypassed, and the lower expansion process is assumed to operate isenthalpically.

The transcritical mode is more complex. Subcooling cannot be applied because the gas cooler pressure exceeds the critical point. Consequently, the gas cooler outlet state is determined by assuming the pinch point of the gas cooling process is there. This is necessary to achieve the maximum COP, as was explained by Liu et al. [17].

The next step is to determine the intermediate pressure after the upper expansion valve, P_{int}. At steady state, the valve outlet must lie on the boiling line. Assuming the receiver outlet is a saturated liquid and neglecting heat losses, the valve outlet must also be saturated liquid as seen from imposing an energy balance on the receiver. Calculating the corresponding liquid saturation pressure for a given enthalpy is non-trivial for refrigerant mixtures. Therefore, a solver iteratively adjusts P_{int} until the enthalpy of saturated liquid at P_{int} equals the enthalpy of the expansion valve inlet. With an isenthalpic expansion in the lower expansion valve, the cycle continues like in subcritical mode. The calculation scheme for the transcritical cycle is summarized in Table 4.

Table 4. Calculation scheme for the transcritical HTHP model. State point numbers are according to Fig. 1.

State point	**Variable 1**	**Variable 2**
1	$P_1 = P_{\mathrm{suc}}$	$T_1 = T_9$
2	$P_2 = P_{\mathrm{dis}}$	$h_2 = h_1 + (h(P_2, s_1) - h_1)/\eta_{\mathrm{ois}} \cdot (1 - \zeta_{\mathrm{co}})$
3	$P_3 = P_{\mathrm{dis}} + \Delta P_{23}$	$h_3 = h_2$
4	$P_4 = P_{\mathrm{dis}} + \Delta P_{24}$	$h_4 = h_3$
5	$P_5 = P_{\mathrm{dis}} + \Delta P_{25}$	$T_5 = T_{\mathrm{si,in}} + \Delta T_{\mathrm{pp,gc}}$
6	$P_6 = P_{\mathrm{int}}$	$h_6 = h(P_6, x = 0)$
7	$P_7 = P_6$	$h_7 = h_6$
8	$P_8 = P_{\mathrm{suc}} + \Delta P_{81}$	$h_8 = h_7$
9	$P_9 = P_{\mathrm{suc}} + \Delta P_{91}$	$T_9 = T(P_9, x = 1) + \Delta T_{\mathrm{sh}}$

2.3. Application example

In this study, the test conditions were selected based on an industrial application suitable for the transcritical HTHP. In the coffee drying process, hot air at a temperature of at least 150 °C is needed [18]. During the drying process, this air is cooled down to 90 °C, as indicated in Fig. 2. The coffee drying effluents are utilized as the heat source for the heat pump, cooling them down further to 60 °C. Consequently, the transcritical HTHP operates with a heat sink inlet temperature of 100 °C and a heat source inlet temperature of 90 °C, while the heat sink outlet and heat source outlet temperatures are 150 °C and 60 °C, respectively.

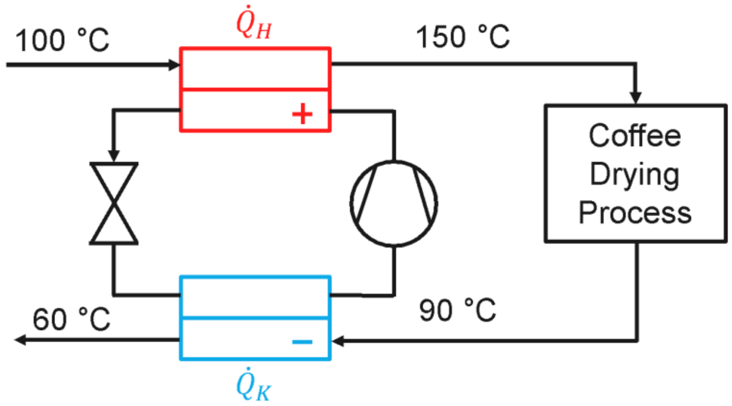

Figure 2. Flow chart of the transcritical HTHP supplying hot air to a coffee drying process.

3. Results and Discussion

For the chosen heat sink and source temperatures, the simulation model was used to determine the most-promising pure refrigerant and refrigerant mixture to achieve the highest COP. The present study focused on hydrocarbons due to their environmental friendliness. The hydrocarbons propane (R-290), isobutane (R-600a), butane (R-600), and isopentane (R-601a) were analyzed.

According to the model results, the best pure refrigerant is R-600a, promising the highest COP for the chosen sink and source temperatures. Among the possible binary mixture compositions, the highest COP could be achieved with a mixture of R-290 and R-601a. The reason for this is the large temperature glide of the mixture.

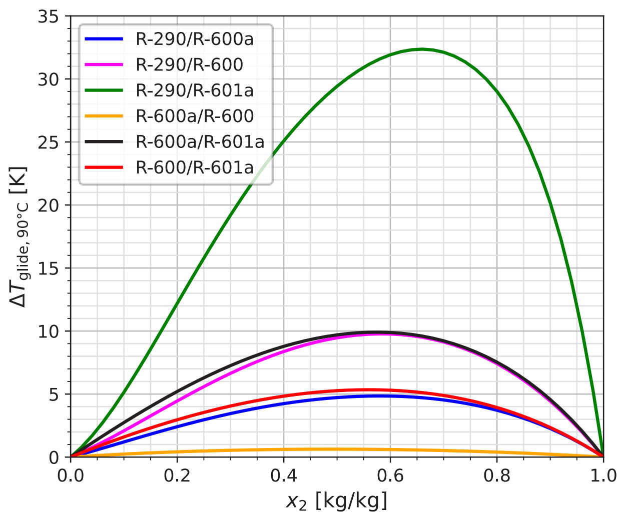

Figure 3: Temperature glide at a dew point temperature of 90 °C as a function of mass fraction of the second component for various hydrocarbon mixtures.

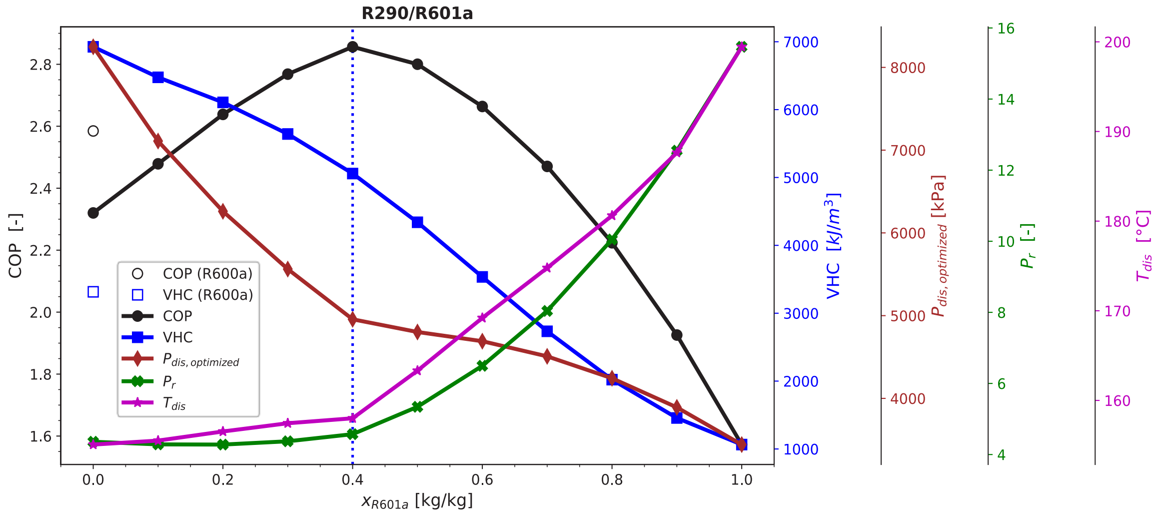

Figure 4. COP, VHC, discharge pressure, pressure ratio, and discharge temperature as functions of the mass fraction of R-601a in a mixture with R-290. For comparison, the COP and VHC of pure R-600a are shown as hollow circle and square, respectively.

This is exemplified in Fig. 3, showing the temperature glide at a dew point temperature of 90 °C, $\Delta T_{\mathrm{glide,90°C}}$, as a function of the mass fraction of the second component for the analyzed hydrocarbon mixtures. $\Delta T_{\mathrm{glide,90°C}}$ was calculated with Equation (1), where $P_{\mathrm{dew,90°C}}$ is the dew point pressure at 90 °C and T_{bubble} is the respective bubble point temperature at this pressure.

$$\Delta T_{\mathrm{glide,90°C}} = 90\ \mathrm{°C} - T_{\mathrm{bubble}}(P_{\mathrm{dew,90°C}}) \tag{1}$$

Fig. 3 shows that the mixture of R-290 and R-601a has the largest range of possible temperature glides. Therefore, the temperature profile of the evaporating refrigerant can be matched best to the heat source temperature profile of the application, explaining the highest possible COP among the analyzed mixtures.

The model results of the best pure refrigerant (R-600a) and the best mixture (R-290 with R-601a) are compared in Fig. 4. A maximum COP of about 2.85 is obtained for a mixture of 60% R-290 and 40% R-601a (w/w), resulting in a COP increase of over 10% compared to pure R-600a (COP of 2.58, hollow circle in Fig. 4). This improvement can be mainly attributed to the near-perfect glide matching during evaporation, as illustrated in the T-s diagrams depicted in Fig. 5. The glide matching raises the suction pressure, reduces the pressure ratio, and consequently increases the COP.

Another important evaluation parameter of a heat pump is the volumetric heating capacity (VHC). It is calculated with Equation (2), where η_{vol} is the volumetric efficiency of the compressor, ρ_{suc} is the suction gas density, and $h_{\mathrm{gc,in}}$ and $h_{\mathrm{gc,out}}$ are the enthalpies at gas cooler inlet and outlet, respectively.

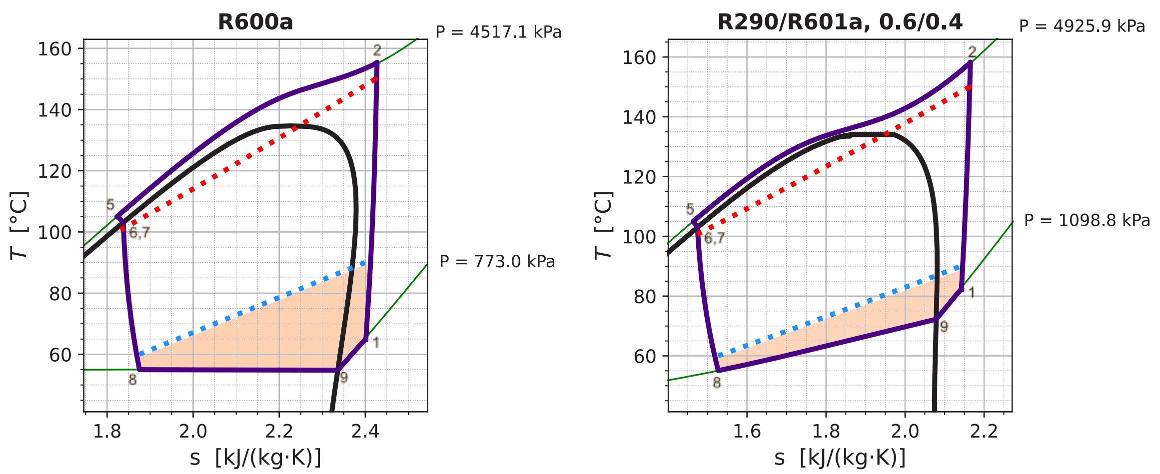

Figure 5. T-s-diagrams of R-600a and the R-290/R-601a mixture (60%/40%, w/w) with the highest COP. Orange-marked areas represent exergy losses in the evaporator. State point numbers are according to Table 4.

$$\mathrm{VHC} = \eta_{\mathrm{vol}} \cdot \rho_{\mathrm{suc}} \cdot \left(h_{\mathrm{gc,in}} - h_{\mathrm{gc,out}}\right) \quad (2)$$

Although the mixture composition that shows the largest COP does not achieve the highest VHC (see Fig. 4), it still exhibits a VHC improvement of more than 50% over pure R-600a (hollow square in Fig. 4). A higher VHC allows the heat pump to deliver more heat to the heat sink with the same compressor, or alternatively, meet the same heat demand with a smaller compressor, reducing investment cost.

The optimized discharge pressure decreases with increasing mass fraction of R-601a because it has a lower critical pressure than R-290. Under the pinch point condition at the gas cooler outlet, the resulting pressure of the temperature $T_{\mathrm{si,in}} + \Delta T_{\mathrm{pp,gc}}$ is lower for R-601a than for R-290. While higher R-601a mass fractions reduce the optimized discharge pressure, they increase the pressure ratio, resulting in higher discharge temperatures. Consequently, feasible mixture compositions are limited by the maximum allowable temperatures and pressures of the available components.

4. Conclusions

This study presents a customized 20-kW transcritical high-temperature heat pump (HTHP) prototype for hydrocarbon refrigerant mixtures. Using a tailored simulation model, the performance of the pure refrigerant isobutane (R-600a) was compared to mixtures of propane (R-290) and isopentane (R-601a) for an application example with heat source inlet and outlet temperatures of 90 °C and 60 °C and heat sink inlet and outlet temperatures of 100 °C and 150 °C, respectively. The model predicts that a 60 wt.-% R-290 / 40 wt.-% R-601a mixture achieves the highest COP, improving it by over 10% compared to pure R-600a, while also increasing the volumetric heating capacity (VHC) by more than 50%. This allows more heat to be supplied to the heat sink medium using the same compressor. To validate these theoretical results, experiments will be conducted on the transcritical HTHP prototype presented here. Additional experimental data will enable refinement of the simulation model and a potential scale-up for designing a pilot plant in an industrial setting.

Acknowledgements

The authors gratefully acknowledge the financial support of the Swiss National Science Foundation and Innosuisse (Bridge Discovery project with grant number 203645), as well as the Swiss Federal Office of Energy (SFOE) for the projects IEA HPT TCP Annex 59 – Heat Pumps for Drying (SI/502606) and SWEET DeCarbCH (SI/502260, www.sweet-decarb.ch).

References

[1] Arpagaus, C., Bless, F., Uhlmann, M., Schiffmann, J., & Bertsch, S. S. (2018). High temperature heat pumps: Market overview, state of the art, research status, refrigerants, and application potentials. Energy, 152, 985-1010, https://doi.org/10.1016/j.energy.2018.03.166.

[2] Arpagaus, C., Bless, F., & Bertsch, S. S. (2020). Theoretical analysis of transcritical HTHP cycles with low GWP HFO refrigerants and hydrocarbons for process heat up to 200 °C. In Proceedings of the IIR Rankine Conference 2020, 26-29 July 2020, Glasgow, UK, http://dx.doi.org/10.18462/iir.rankine.2020.1168.

[3] Udroiu, C. M., Navarro-Esbrí, J., Giménez-Prades, P., & Mota-Babiloni, A. (2024). Towards sustainable process heating at 250° C: Modeling and optimization of an R1336mzz (Z) transcritical High-Temperature heat pump. Applied Thermal Engineering, 242, 122521, https://doi.org/10.1016/j.applthermaleng.2024.122521.

[4] Vieren, E., Demeester, T., Beyne, W., Arteconi, A., De Paepe, M., & Lecompte, S. (2023). The thermodynamic potential of high-temperature transcritical heat pump cycles for industrial processes with large temperature glides. Applied Thermal Engineering, 234, 121197, https://doi.org/10.1016/j.applthermaleng.2023.121197.

[5] Zhao, A., Pecnik, R., & Peeters, J. W. (2024). Thermodynamic analysis and heat exchanger calculations of transcritical high-temperature heat pumps. Energy Conversion and Management, 303, 118172, https://doi.org/10.1016/j.enconman.2024.118172.

[6] Besbes, K., Zoughaib, A., Carlan, F. D., & Peureux, J. L. (2015). A R-32 transcritical heat pump for high temperature industrial applications. In Proceedings of the 24th IIR International Congress of Refrigeration, ICR-2015, http://dx.doi.org/10.18462/iir.icr.2015.0599.

[7] Abi Chahla, G., Beucher, Y., Zoughaib, A., De Carlan, F., & Pierucci, J. (2019, August). Transcritical industrial heat pump using HFO's for up to 150◦ C hot air supply. In Proceedings of the 25th IIR International Congress of Refrigeration, ICR-2019.

[8] Kimura, T., Fuchikami, H., Nishida, K., Kudo, M., Machida, A., Saito, K., ... & Katsuta, M. (2018). Development of a high temperature heat pump using reusable heat as the heat source. In Jraia international symposium (pp. 1-8), https://waermepumpe-izw.de/wp-content/uploads/2020/05/181206-7-Kobe-Conf-Paper-1046.pdf.

[9] Saito, K. (2017). Latest heat pump technologies in Japan. In 12th IEA Heat Pump Conference (pp. 3-4), https://heatpumpingtechnologies.org/publications/k-4-7-1-latest-heat-pump-technologies-in-japan/

[10] Verdnik, M., Rieberer, R., & Moisi, H. (2019). Trans-critical vapor compression cycle using butane (R600) as refrigerant for industrial waste heat recovery. Refrigeration Science and Technology, 2019, 4697-4704, http://dx.doi.org/10.18462/iir.icr.2019.1186.

[11] Roskosch, D., Venzik, V., & Atakan, B. (2017). Thermodynamic model for reciprocating compressors with the focus on fluid dependent efficiencies. Int. J. Refrig., 84, 104-116, https://doi.org/10.1016/j.ijrefrig.2017.08.011.

[12] Navarro, E., Martinez-Galvan, I. O., Nohales, J., & Gonzálvez-Maciá, J. (2013). Comparative experimental study of an open piston compressor working with R-1234yf, R-134a and R-290. Int. J. Refrig., 36(3), 768-775, https://doi.org/10.1016/j.ijrefrig.2012.11.017.

[13] Kauf, F. (1999). Determination of the optimum high pressure for transcritical CO2-refrigeration cycles. International Journal of Thermal Sciences, 38(4), 325-330, https://doi.org/10.1016/S1290-0729(99)80098-2.

[14] Brendel, L. P., Arpagaus, C., & Bertsch, S. S. (2025). Practical Design Guidelines for High-Glide Mixtures in Industrial Heat Pumps using Hydrocarbon Refrigerants. 31. Tagung des BFE-Forschungsprogramms «Wärmepumpen und Kältetechnik».

[15] Virtanen, P., Gommers, R., Oliphant, T. E., Haberland, M., Reddy, T., Cournapeau, D., ... & Van Mulbregt, P. (2020). SciPy 1.0: fundamental algorithms for scientific computing in Python. Nature methods, 17(3), 261-272, https://doi.org/10.1038/s41592-019-0686-2.

[16] Huber, M., Harvey, A., Lemmon, E., Hardin, G., Bell, I., & McLinden, M. (2018). NIST Reference Fluid Thermodynamic and Transport Properties Database (REFPROP) Version 10 - SRD 23. National Institute of Standards and Technology, https://doi.org/10.18434/T4/1502528.

[17] Liu, R., Gao, F., Liang, K., Wang, L., Wang, M., Mi, G., & Li, Y. (2021). Thermodynamic evaluation of transcritical CO2 heat pump considering temperature matching under the constraint of heat transfer pinch point. Journal of Thermal Science, 30(3), 869-879, https://doi.org/10.1007/s11630-021-1373-z.

[18] Shofinita, D., Lestari, D., Aliwarga, L. et al. (2024): Drying Methods of Coffee Extracts and Their Effects on Physicochemical Properties: A Review. Food Bioprocess Technol 17, 47–72 (2024), https://doi.org/10.1007/s11947-023-03067-4